Computational analysis for energy accumulation and non-axisymmetric features in a shocked spherical bubble

John Niederhaus, **Jason Oakley**,
Mark Anderson, **Riccardo Bonazza**
University of Wisconsin-Madison
bonazza@engr.wisc.edu

Jeffrey Greenough
Lawrence Livermore National Laboratory
greenough1@llnl.gov

November 19, 2006

59th Annual Meeting of the Division of Fluid Dynamics

Tampa Bay, FL

This work is supported by DOE Grant #DE-FG52-03NA00061

The shock-bubble interaction is the unsteady flow generated by the passage of a shock wave over a discrete, round inhomogeneity in the medium of propagation.

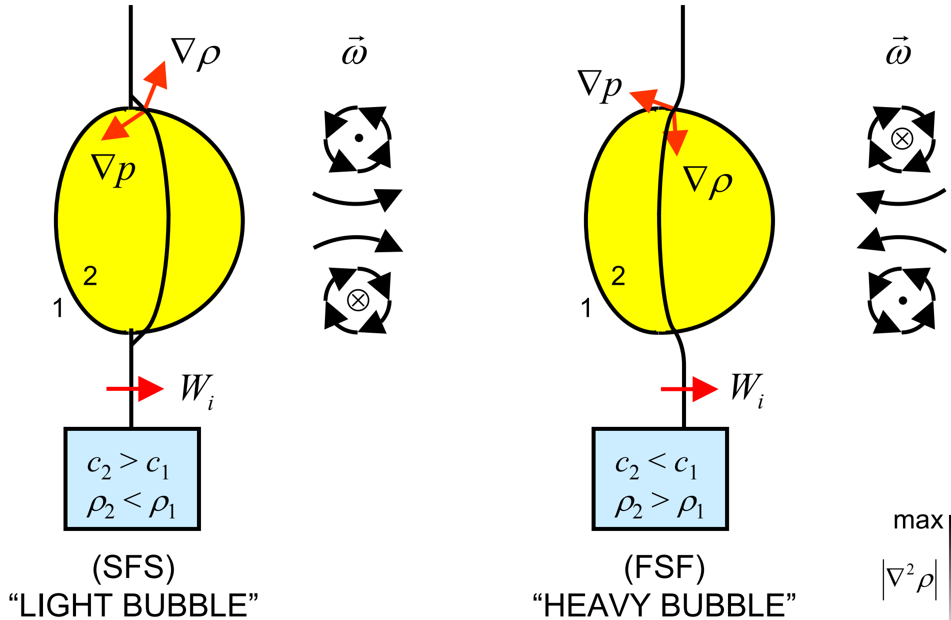

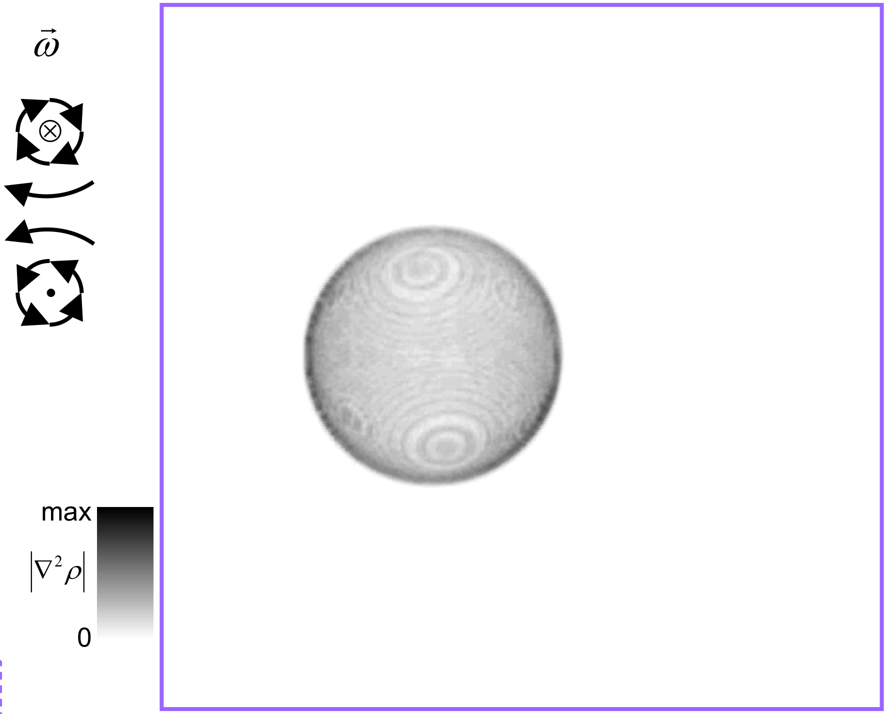

Air-R12, M = 5: 3D rendering of the $|\nabla^2\rho|$ field, attenuated along the line of sight, with isosurfaces of vorticity magnitude in red.

$$\frac{D\vec{\omega}}{Dt} = (\vec{\omega}\cdot\nabla)\vec{V} + \vec{\omega}\left(\nabla\cdot\vec{V}\right) - \nu\nabla^2\vec{\omega} + \underbrace{\frac{1}{\rho^2}(\nabla\rho\times\nabla p)}_{\text{baroclinic}}$$

Nonlinearly-coupled physical processes at work:

- Shock compression
- Nonlinear-acoustic effects
- Vorticity generation and transport

Defining parameters:

$$M = \frac{W_i}{c_1} \qquad A = \frac{\rho_2 - \rho_1}{\rho_1 + \rho_2}$$

Computations for the shock-bubble interaction: scheme and setup

To simulate this problem in 3D, we have used the AMR code, *Raptor* (LLNL):

- 3D compressible Euler equations are solved, with a gamma-law EOS.
- Operator-split, piecewise-linear, second-order Godunov method (Collela, 1985) is employed.
- Integrator is embedded in the block-structured adaptive mesh refinement (AMR) framework of Berger and Oliger (1984) and Rendleman *et al.* (1998)
- Scheme extended to multiple fluids by adopting the VOF method of Miller and Puckett (1996).
- Turbulence treatment is implicit: MILES (monotone-integrated large-eddy simulation).

Initial conditions and boundary conditions:

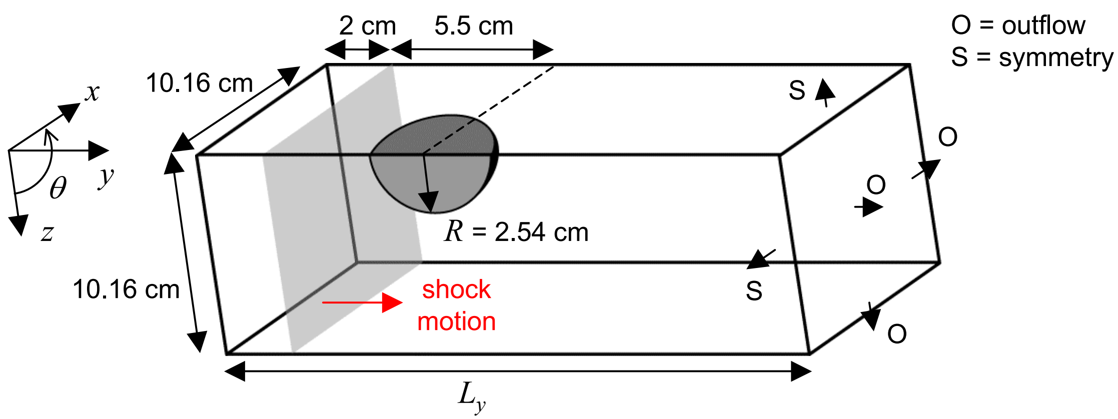

Grid:

- 3D Cartesian mesh
- 2 levels of refinement, 4× each
- Refine on $|\nabla\rho|$ and f
- ¼ symmetry
- Finest level resolution: R_{128} ($\Delta = 198$ μm)
- ~10^7 cells total

$|\nabla\rho|$ = density gradient magnitude

f = bubble fluid volume fraction

Parameter study:

- Mechanical shock tube conditions
- Previously studied in 2D

	A	M
Air-He	-0.757	1.2, 1.5, 1.68
N_2-Ar	0.176	1.33, 2.88, 3.38
Air-Kr	0.486	1.2, 1.5, 1.68
Air-R12	0.613	1.14, 2.5, 5.0

Issues:

- Secondary circulation
- Energy accumulation
- Non-axisymmetric features

Energy accumulation in bubble: convergent vs. divergent configuration

Bubble internal energy: $$E_2(t) = \iiint_D \rho\, g_2 \left[e - \tfrac{1}{2}\left(u^2 + v^2 + w^2\right)\right] dV$$ → Difference between total and kinetic energy in fluid 2 at time t.

g_2 = fluid-2 mass fraction, ρ = total density, e = total energy per unit mass, $[u, v, w]$ = fluid velocity

Normalization:

$$\tilde{E}_2(t) \equiv \frac{E_2(t) - E_2(0)}{E_f^{1D} - E_2(0)}$$

$$E_f^{1D} = c_V T_f^{1D} = \frac{R T_f^{1D}}{\gamma - 1}$$

Solve 1D gasdynamics equations recursively for shock reflection/transmission events in gas slab to find T_f^{1D}

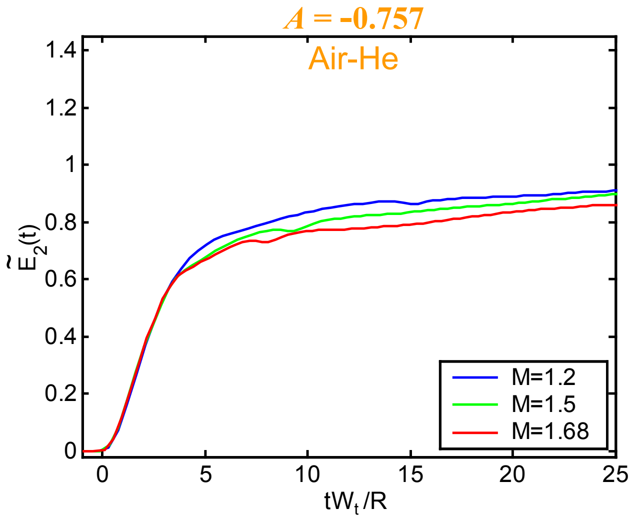

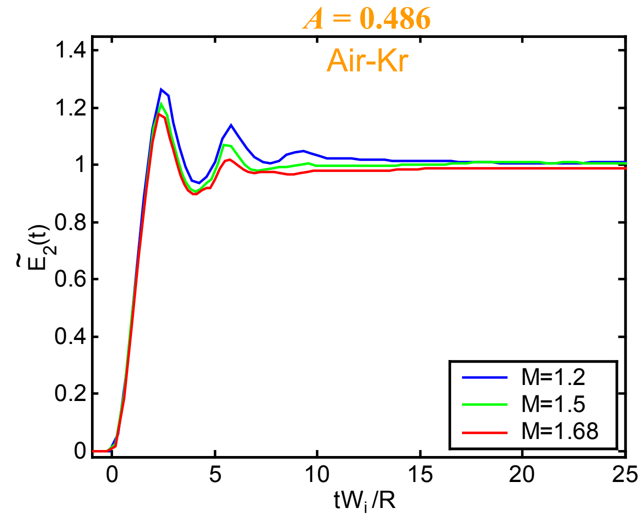

- Energy accumulation in the bubble fluid becomes non-monotonic in time for $A > 0$
- Oscillatory behavior of internal energy arises because of convergent geometry.

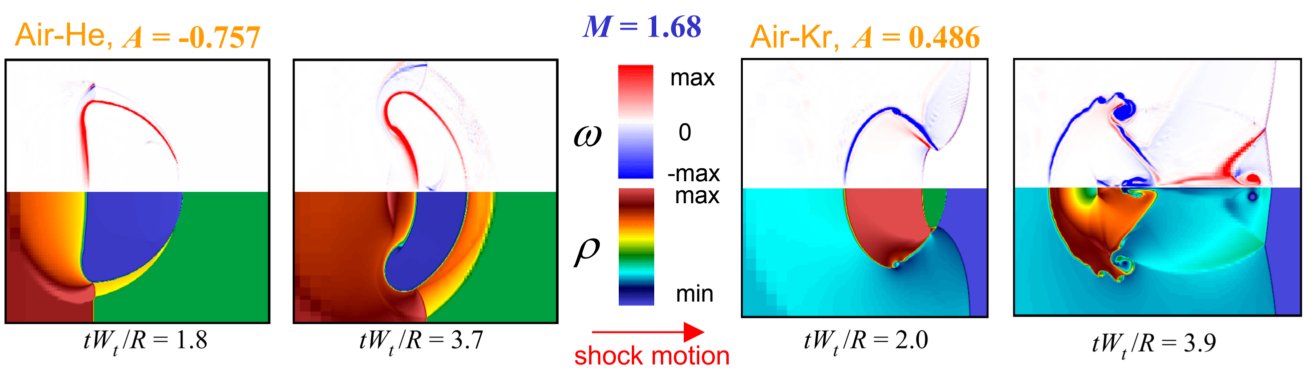

$tW_t/R = 1.8$ $tW_t/R = 3.7$ $tW_t/R = 2.0$ $tW_t/R = 3.9$

W_t = transmitted shock wave speed

Energy accumulation in bubble: convergent vs. divergent configuration

Bubble mean density:

$$\rho^*(t) = \frac{1}{3}\pi R^3 \rho_2 \left(\iiint_D f_2 \, dV \right)^{-1}$$

→ Mean density of fluid 2 at time t.

f_2 = fluid-2 volume fraction, ρ_2 = initial bubble fluid density,

Normalization:

$$\tilde{\rho}^*(t) \equiv \frac{\rho^*(t) - \rho_2}{\rho_f^{1D} - \rho_2}$$

Solve 1D gasdynamics equations recursively for shock reflection/transmission events in gas slab to find ρ_f^{1D}

A = -0.757

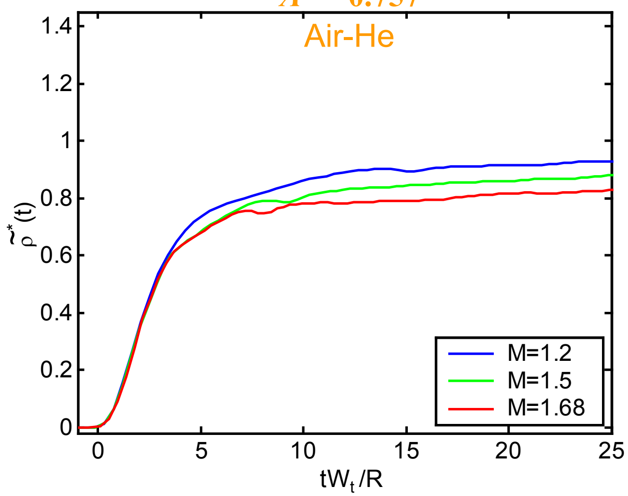

A = 0.486

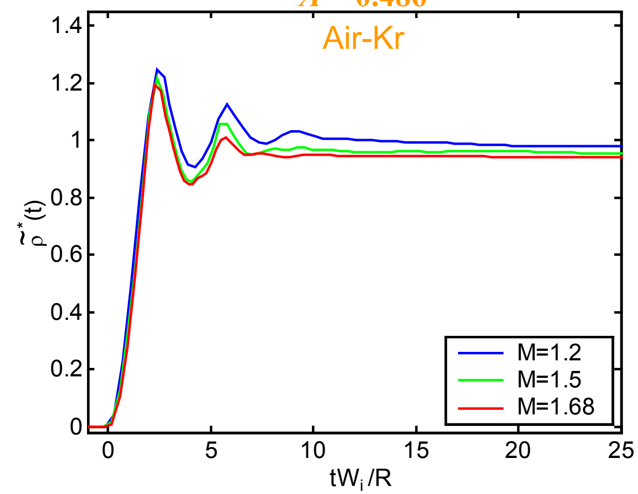

The non-monotonic accumulation of internal energy in the bubble fluid for $A > 0$ manifests itself in the mean density of the bubble fluid.

Air-He, A = -0.757

M = 1.68

Air-Kr, A = 0.486

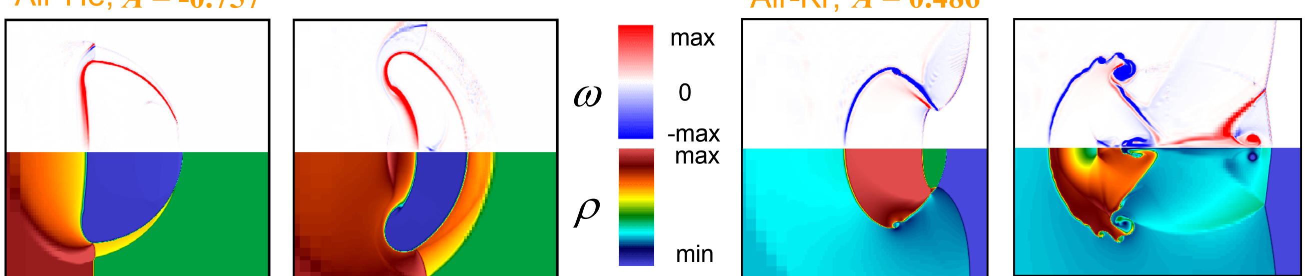

$tW_t/R = 1.8$ $tW_t/R = 3.7$ shock motion $tW_i/R = 2.0$ $tW_i/R = 3.9$

W_t = transmitted shock wave speed

W_i = incident shock wave speed

Energy accumulation in bubble: non-monotonicity in time for $A > 0$

Bubble mean density:

$$\rho^*(t) = \frac{1}{3}\pi R^3 \rho_2 \left(\iiint_D f_2 \, dV \right)^{-1}$$

→ Mean density of fluid 2 at time t.

f_2 = fluid-2 volume fraction, ρ_2 = initial bubble fluid density,

Normalization:

$$\tilde{\rho}^*(t) \equiv \frac{\rho^*(t) - \rho_2}{\rho_f^{1D} - \rho_2}$$

Solve 1D gasdynamics equations recursively for shock reflection/transmission events in gas slab to find ρ_f^{1D}

The non-monotonic accumulation of internal energy in the bubble fluid for $A > 0$ manifests itself in the mean density of the bubble fluid.

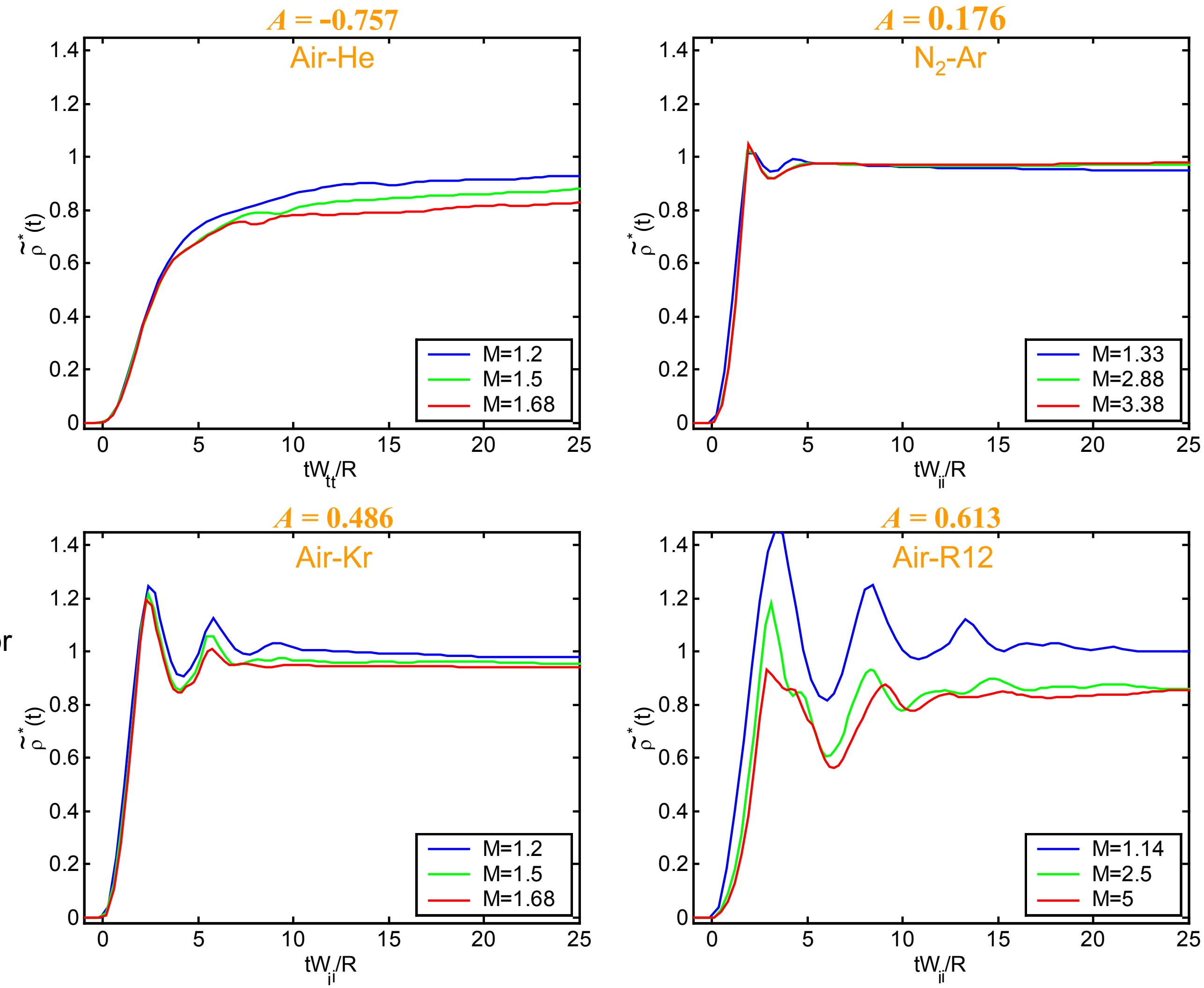

Energy accumulation in bubble: non-monotonicity in time for $A > 0$

Non-monotonic accumulation of bubble fluid internal energy is driven by the $\nabla \cdot \vec{V}$ field, which appears in the evolution equation for internal energy:

$$\frac{\partial}{\partial t} E + (\nabla \cdot E)\vec{V} + p\left(\nabla \cdot \vec{V}\right) = 0$$

compression / expansion (departure from incompressibility)

E = internal energy per unit volume

Integrate the $\nabla \cdot \vec{V}$ contribution over the bubble fluid volume for $A > 0$, $A < 0$ at fixed M:

$$Q(t) = \iiint_D \delta(g_2) p \left(\nabla \cdot \vec{V}\right) dV = 0 \qquad \delta(g_2) = \begin{cases} 1, & g_2 \geq 10^{-7} \\ 0, & \text{else} \end{cases}$$

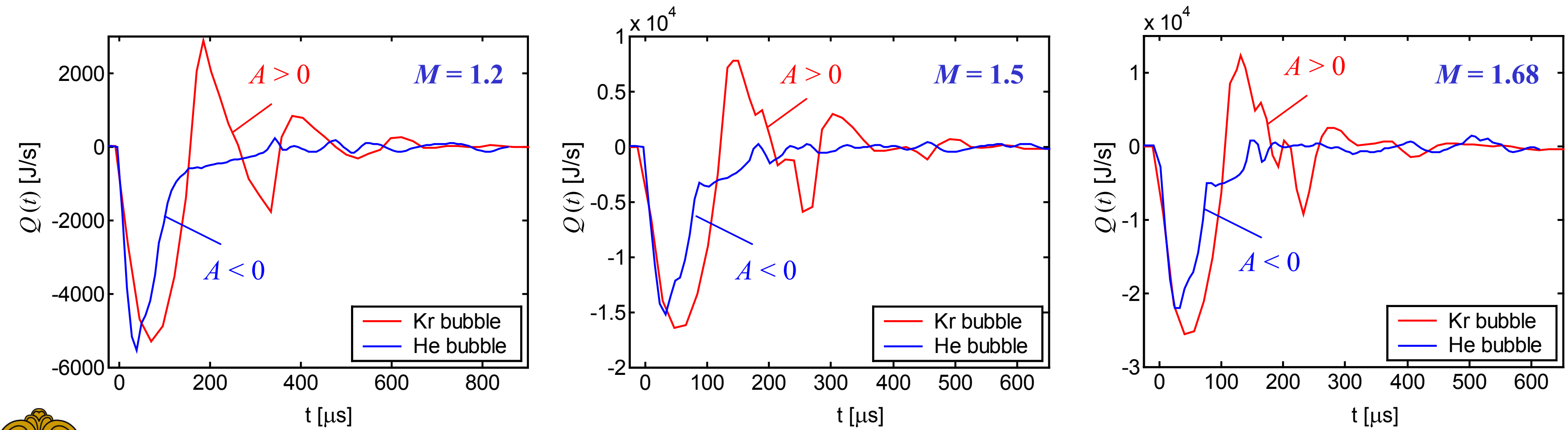

The convergent geometry associated with A > 0 introduces oscillatory behavior into the energy accumulation, via reflected rarefactions and reflected shocks.

Non-axisymmetric features: strong turbulence-like effects for high $A > 0.2$

Parameter study results indicate turbulence-like features are significant at late times for $A > 0.2$.

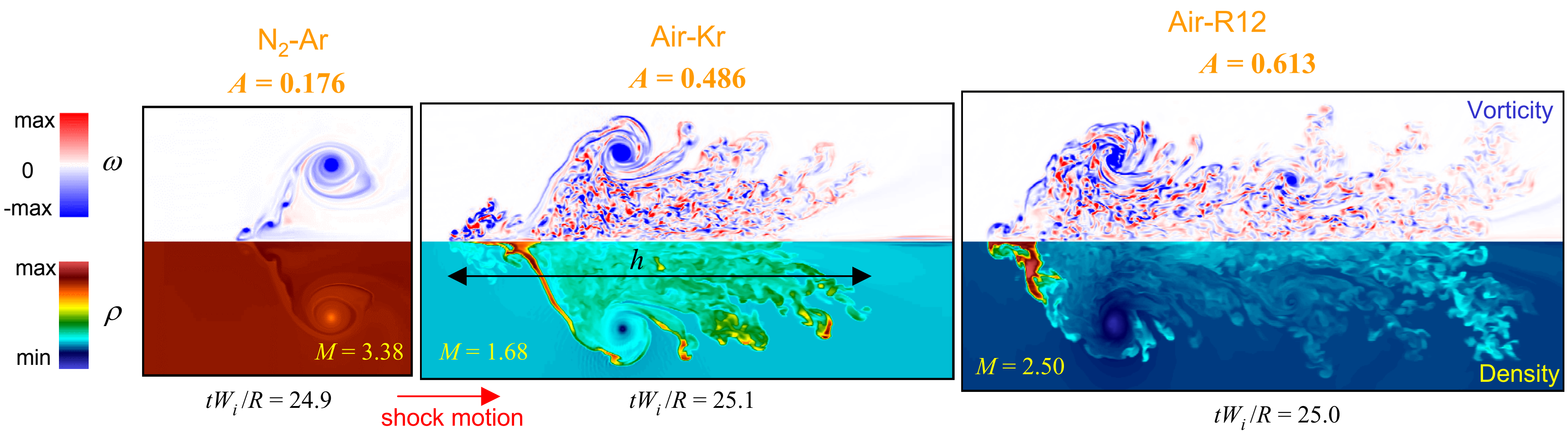

These features cannot be described as "turbulent":

- Simulation is inviscid.
- No explicit turbulence model is in place.
- Implicit numerical dissipation acts at scales of $\Delta \sim 10^{-4}$ m, but the physical dissipative scale is $\eta \sim 10^{-6}$ m.
- The effective Reynolds number* is low:

$$\mathrm{Re}_h = \left(\frac{h}{\Delta}\right)^{4/3} \sim 10^3$$

However, they possess many features typically attributed to turbulence:

- Disordered/chaotic state arises, particularly apparent in the vorticity field.
- Transport and mixing phenomena are enhanced.
- A wide range of length scales is evident.
- Reynolds numbers for the viscous analog are high:

$$\mathrm{Re}_\nu = \frac{\Gamma}{\nu} \sim 10^5$$

* A.R. Miles, Ph.D. thesis, Univ. of Maryland, 2004.

Non-axisymmetric fluctuations may be characterized by use of an azimuthal averaging scheme:

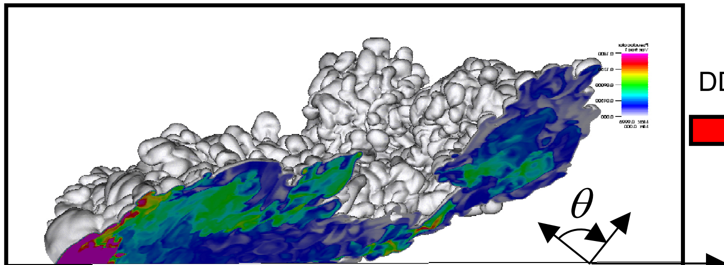

θ = azimuthal coordinate

Raw 3D dataset: $f(x,y,z) \rightarrow f(r,\theta,z)$

DDF

Reynolds averages with respect to θ:

$$\langle f \rangle (r,z) = \frac{2}{\pi} \int_0^{\pi/2} f(r,\theta,z)\, d\theta \qquad \tilde{f}(r,z) = \frac{2}{\pi} \sqrt{\int_0^{\pi/2} \left(f(r,\theta,z) - \langle f \rangle (r,z) \right)^2 d\theta}$$

Mean

Standard deviation

Intensity of fluctuations:

$$\hat{\tilde{f}}(t) = \frac{\int_0^{r_1} \int_{z_1}^{z_2} \tilde{f}(r,z)\, dz\, dr}{r_1 (z_2 - z_1)}$$

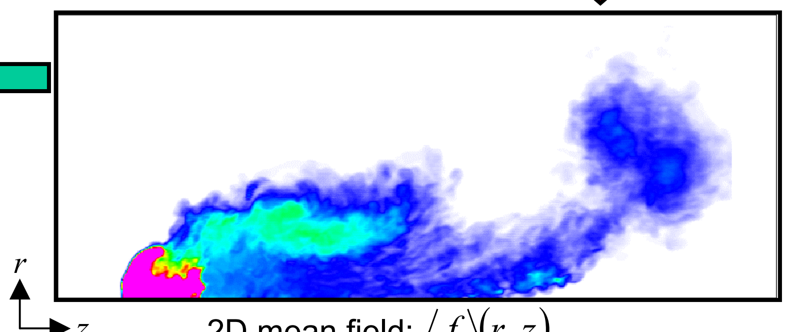

2D mean field: $\langle f \rangle (r,z)$

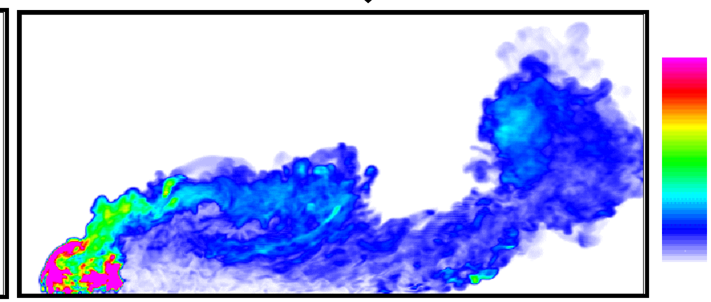

2D field of RMS fluctuations: $\tilde{f}(r,z)$

Radial profiles of z-averaged fluctuations. $\bar{\tilde{f}}(r) = (z_2 - z_1)^{-1} \int_{z_1}^{z_2} \tilde{f}(r,z)\, dz$

Axial profiles of r-averaged fluctuations. $\bar{\bar{\tilde{f}}}(z) = r_1^{-1} \int_0^{r_1} \tilde{f}(r,z)\, dr$

Apply Fourier analysis:

$$F_f^r(k_r) = \mathrm{FT}\left[\bar{\tilde{f}}(r)\right]$$

$$F_f^z(k_z) = \mathrm{FT}\left[\bar{\bar{\tilde{f}}}(z)\right]$$

Non-axisymmetric features: fluctuation intensity dramatically higher for |A| > 0.2

Non-axisymmetric fluctuations are stronger at late times for $A > 0.2$.

Kinetic energy per unit mass

$$K = \frac{1}{2}\left(u^2 + v^2 + w^2\right)$$

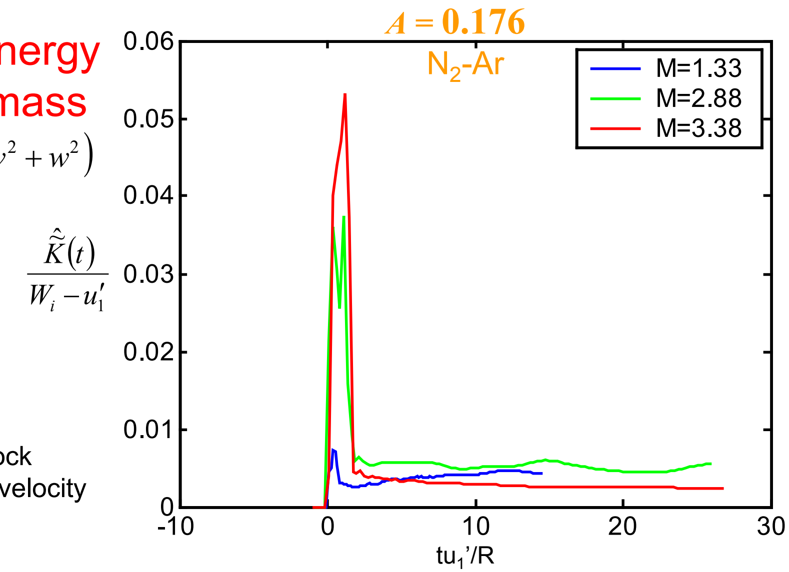

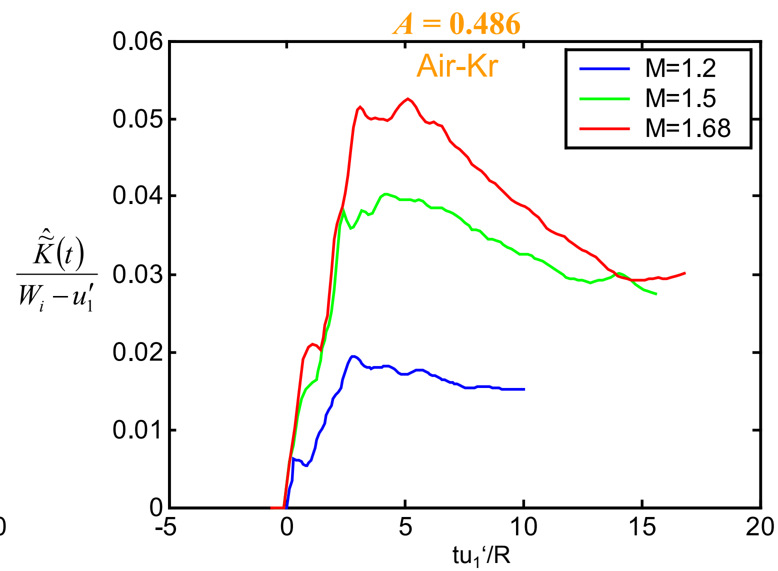

u_1' = post-shock particle velocity in fluid 1

Enstrophy

$$\Omega = \omega^2$$

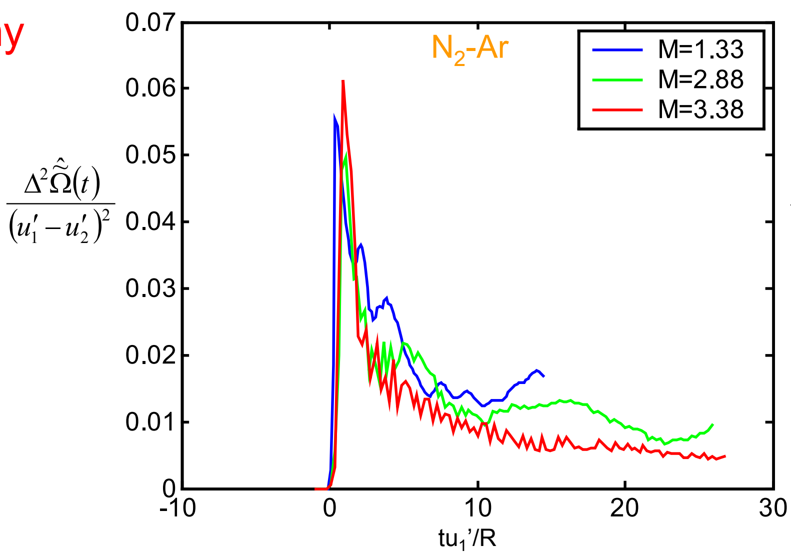

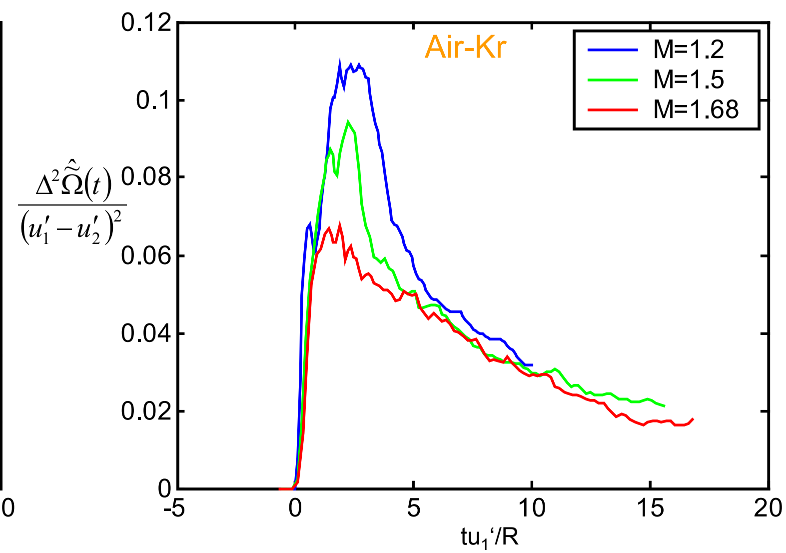

Non-axisymmetric features: qualitative and spectral analysis of fluctuating fields

Fluctuations in K and Ω for the highest Atwood-number scenario: air-R12, M = 5.0 (A = 0.613)

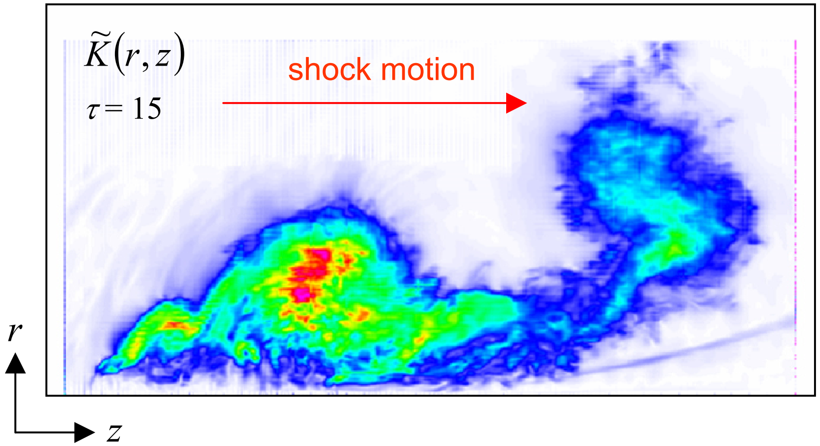

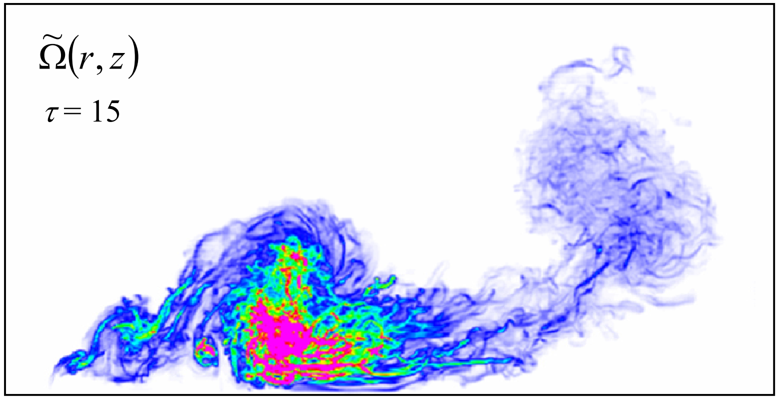

Fourier spectra of z-averaged fluctuations in K and W

$$\tau = \frac{tu_1'}{R}$$

u_1' = post-shock particle velocity in fluid 1

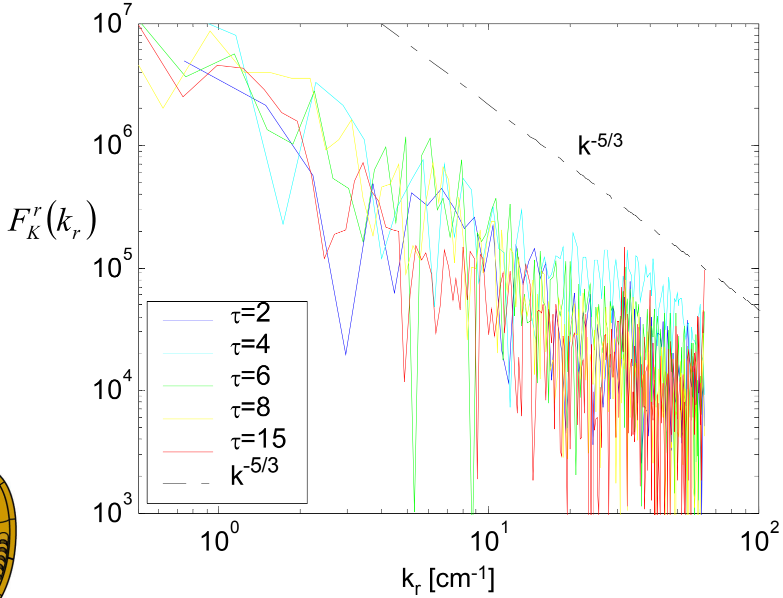

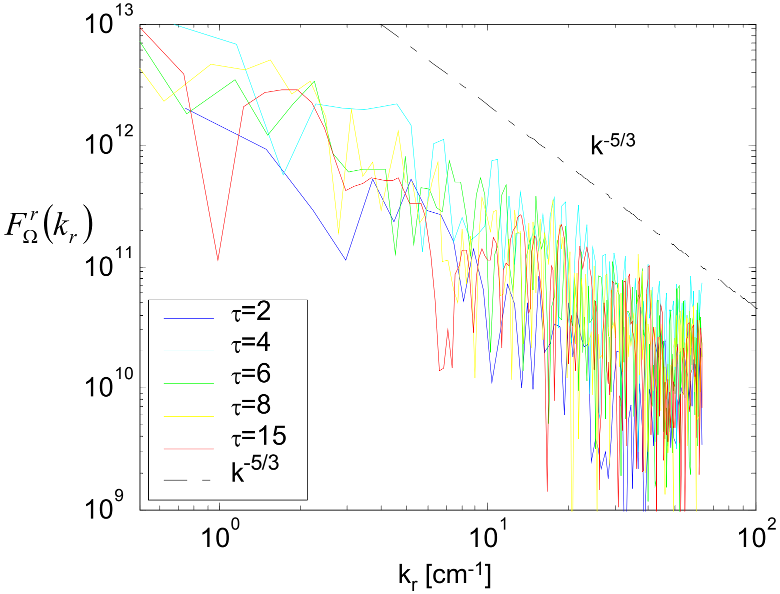

Conclusions

- A computational parameter study has been performed in 3D for the shock-bubble interaction, including 12 realizations.
- Integral diagnostics on the resulting databases have yielded insights into the shock-induced compression, circulation, interface distortion, and mixing phenomena.
- An azimuthal averaging scheme has been defined for characterizing turbulence-like features and computing statistical quantities.
- By means of these tools, the study has shed light on more subtle features:
  - Energy accumulation in the bubble becomes non-monotonic in time for $A > 0$.
  - Non-axisymmetric, turbulence-like features persist at late times for $A > 0.2$.

R12 bubble in air
At = 0.613
$M = 5.0$

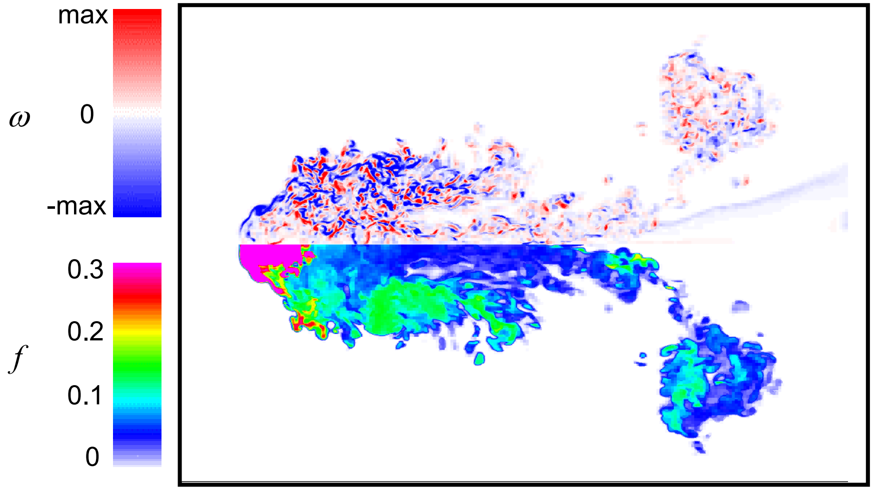

For more flow visualizations from these simulations, take a moment to view video # 40 in the Gallery of Fluid Motion, entitled **"Shock-Bubble Interaction"**